NASA/TM—2018–219849

Sandwich Structure Risk Reduction in Support of the Payload Adapter Fitting

A.T. Nettles, J.R. Jackson, and W.E. Guin
Marshall Space Flight Center, Huntsville, Alabama

February 2018

The NASA STI Program…in Profile

Since its founding, NASA has been dedicated to the advancement of aeronautics and space science. The NASA Scientific and Technical Information (STI) Program Office plays a key part in helping NASA maintain this important role.

The NASA STI Program Office is operated by Langley Research Center, the lead center for NASA's scientific and technical information. The NASA STI Program Office provides access to the NASA STI Database, the largest collection of aeronautical and space science STI in the world. The Program Office is also NASA's institutional mechanism for disseminating the results of its research and development activities. These results are published by NASA in the NASA STI Report Series, which includes the following report types:

- TECHNICAL PUBLICATION. Reports of completed research or a major significant phase of research that present the results of NASA programs and include extensive data or theoretical analysis. Includes compilations of significant scientific and technical data and information deemed to be of continuing reference value. NASA's counterpart of peer-reviewed formal professional papers but has less stringent limitations on manuscript length and extent of graphic presentations.

- TECHNICAL MEMORANDUM. Scientific and technical findings that are preliminary or of specialized interest, e.g., quick release reports, working papers, and bibliographies that contain minimal annotation. Does not contain extensive analysis.

- CONTRACTOR REPORT. Scientific and technical findings by NASA-sponsored contractors and grantees.

- CONFERENCE PUBLICATION. Collected papers from scientific and technical conferences, symposia, seminars, or other meetings sponsored or cosponsored by NASA.

- SPECIAL PUBLICATION. Scientific, technical, or historical information from NASA programs, projects, and mission, often concerned with subjects having substantial public interest.

- TECHNICAL TRANSLATION. English-language translations of foreign scientific and technical material pertinent to NASA's mission.

Specialized services that complement the STI Program Office's diverse offerings include creating custom thesauri, building customized databases, organizing and publishing research results…even providing videos.

For more information about the NASA STI Program Office, see the following:

- Access the NASA STI program home page at <http://www.sti.nasa.gov>

- E-mail your question via the Internet to <help@sti.nasa.gov>

- Phone the NASA STI Help Desk at 757–864–9658

- Write to:
  NASA STI Information Desk
  Mail Stop 148
  NASA Langley Research Center
  Hampton, VA 23681–2199, USA

NASA/TM—2018–219849

Sandwich Structure Risk Reduction in Support of the Payload Adapter Fitting

A.T. Nettles, J.R. Jackson, and W.E. Guin
Marshall Space Flight Center, Huntsville, Alabama

National Aeronautics and
Space Administration

Marshall Space Flight Center • Huntsville, Alabama 35812

February 2018

TRADEMARKS

Available from:

NASA STI Information Desk
Mail Stop 148
NASA Langley Research Center
Hampton, VA 23681–2199, USA
757–864–9658

This report is also available in electronic form at
<http://www.sti.nasa.gov>

TABLE OF CONTENTS

LIST OF FIGURES

LIST OF FIGURES (Continued)

LIST OF TABLES

LIST OF ACRONYMS

BVID	barely visible impact damage
CAI	compression after impact
DTA	damage threat assessment
FAA	Federal Aviation Administration
FOD	foreign object debris
FWCF	finite width correction factor
NDE	nondestructive evaluation
OHC	open hole compression
OoA	out-of-autoclave

NOMENCLATURE

d	diameter
r	radius of hole (or damage)
w	panel width
σ	stress
σ_{app}	applied stress at ends of panel
σ_{hole}	increased stress at edge of hole

TECHNICAL MEMORANDUM

SANDWICH STRUCTURE RISK REDUCTION IN SUPPORT OF THE PAYLOAD ADAPTER FITTING

1. DESIGN TO WHAT?

Unlike airplanes, launch vehicles are never flown with known detrimental damage. This greatly reduces the damage tolerance risk. Launch vehicle hardware can be (and is) much better protected and carefully handled than aircraft hardware. This is true regardless of what material(s) of which the launch vehicle is made. One of the authors (Jackson) has firsthand experience dealing with the aluminum external tank of the space shuttle. Guessing what kinds of damage might occur was impossible; thus as anomalous events arose, they were dispositioned on an individual basis.

A damage threat assessment (DTA) is stated to be done for all man-rated launch vehicles. The definition of a DTA in the composites industry has been the subject of discussion at CMH-17 Handbook meetings for as long as one of the authors (Nettles) can remember and comes exclusively from the aircraft industry that must fly damaged hardware for either economical or practical considerations. It is fully expected that airplanes will be impacted quite often by foreign objects, and they are designed as such based on a DTA. In fact, critical airplane parts are designed to withstand complete-through penetrations due to shrapnel from engine turbine explosions. If flight with no damage is possible (as with launch vehicles), a DTA is not of value. If a threat is identified, then eliminate the threat rather than fly with damage. Airplanes cannot do this; launch vehicle hardware can. At any rate, this is a ground operations problem, and composite laminates are no more prone to impact damage than some of the aluminum-lithium alloys used; thus hardware should not sustain damage, regardless of the material of which it is made.

This leaves the question of how the hardware can be damaged such that the damage is not visible/detectable and is launched with the damage. Some mitigating techniques, such as a highly reflective surface finish and even white light scanning can be used to detect the smallest of impacts. With modern toughened epoxy resins, it is difficult to inflict detrimental damage (lowering of strength to below-limit loads) to a composite laminate without some form of visible damage. The only exception is if permeability is an issue, then nonvisible impacts may cause small leak paths for fluids. Thus, using barely visible impact damage (BVID) is a very conservative technique for launch vehicle hardware. In order to obtain the lightest weight structure and lower risk, white light scanning or another technique that can detect surface anomalies—even those that do not cause damage—can be used.

2. WHAT SIZE SPECIMENS?

This section addresses the issue of test panel size for compression-after-impact (CAI) testing of honeycomb sandwich structure. CAI testing determines failure of the material and does not consider global buckling. Global buckling will be briefly mentioned later. More specifically, the following information sheds light on the answer to the question, How large a panel test is needed to obtain the necessary information to assess a full-scale part when material failure is considered? This paper is only intended to address the effects of damage within the acreage of honeycomb sandwich structure and excludes details such as joints, ply drops, etc. This information is of the most value since the vast majority of foreign object impacts will occur in the acreage sections. This section also assumes a large cylinder as the full-scale structure. The problem being addressed is sketched schematically in figure 1. Dimensions in the figure are for example only.

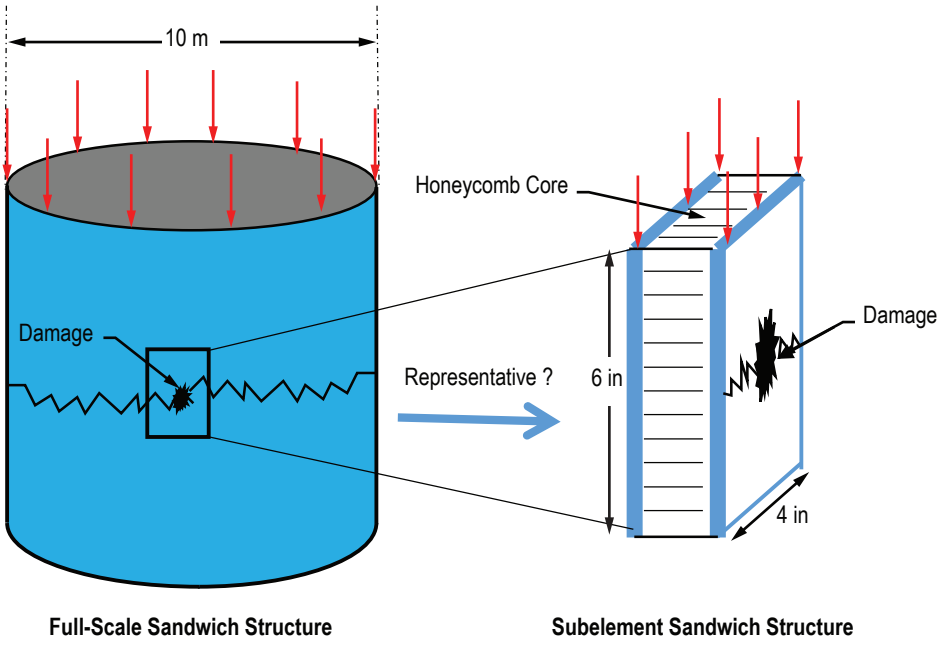

Figure 1. Schematic of problem being addressed in this Technical Memorandum.

Examples based on past tests, conducted at NASA's Marshall Space Flight Center and elsewhere, will be presented to help draw a conclusion as to what size panel is needed to represent the full-scale structure. While the author has no data from actual full-scale hardware tests, which are rarely performed (and all of which is proprietary), trends of CAI strength values from testing sandwich panels of various sizes and curvatures will be presented.

A CAI test actually consists of the following two parts: (1) The infliction of the damage and (2) subsequent load-carrying capability of the damaged sandwich structure. Since the thickness of the subscale panels (test specimens) is the same as the actual test article, this leaves the effects of boundary conditions as the difference in response to an impact for full-scale and subscale testing. This has been looked at previously by the authors of reference 1 and in an FAA report (see ref. 2). Figure 2 is from reference 1 and shows that for the three boundary conditions tested, either method in which the back face of the impacted sandwich structure was rigidly supported over its entire area gave the most damage (as assessed by flash thermography) for a given impact energy level.

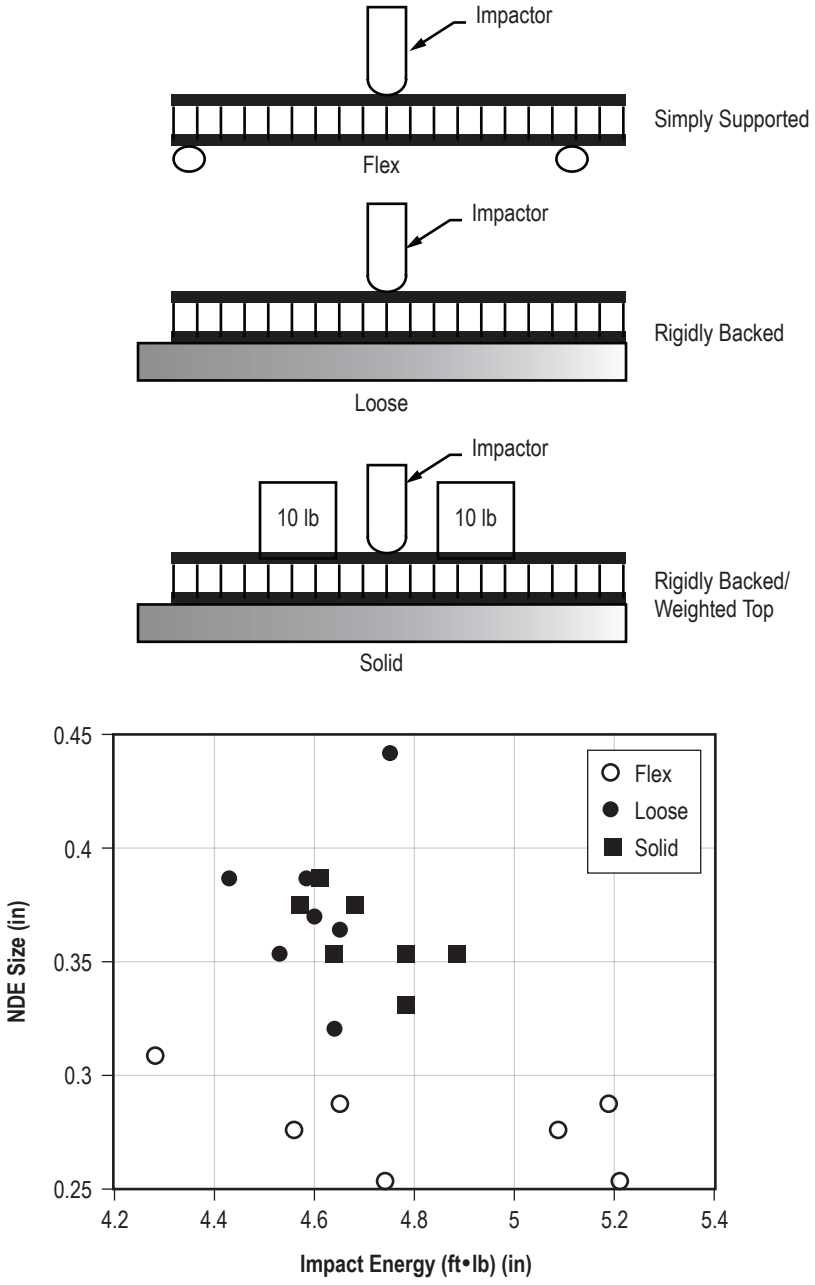

Figure 2. Plot of damage size incurred versus impact energy for three target boundary conditions.[1]

Thus the conclusion was reached that if all sandwich structures were rigidly backed while undergoing impact, then the most damage would be inflicted into the panel, due to any given impact event. Rigidly backed panels cannot flex and absorb elastic energy to help diffuse the energy of the impact; all of the impact energy goes into the form of damage to the panel. This represents a conservative or 'worst-case' scenario for any given impact event. In addition, if all sandwich structures are rigidly backed and not allowed to flex, then all panels would have the same boundary condition regardless of size; whereas, if the panels where simply supported, the amount of damage would depend on the span between the supports.

Figure 3 is from reference 2 and shows something similar to what was found in reference 1. As the impacted sandwich panels are supported such that they are 'stiffer' (less flex allowed), more damage is incurred for a given impact energy. In reference 2, it was concluded that in order to produce repeatable results "…a possible method is to support the back facesheet of the panel over its entire area, thus canceling the effects of global geometry." This is the same conclusion as was obtained in reference 1.

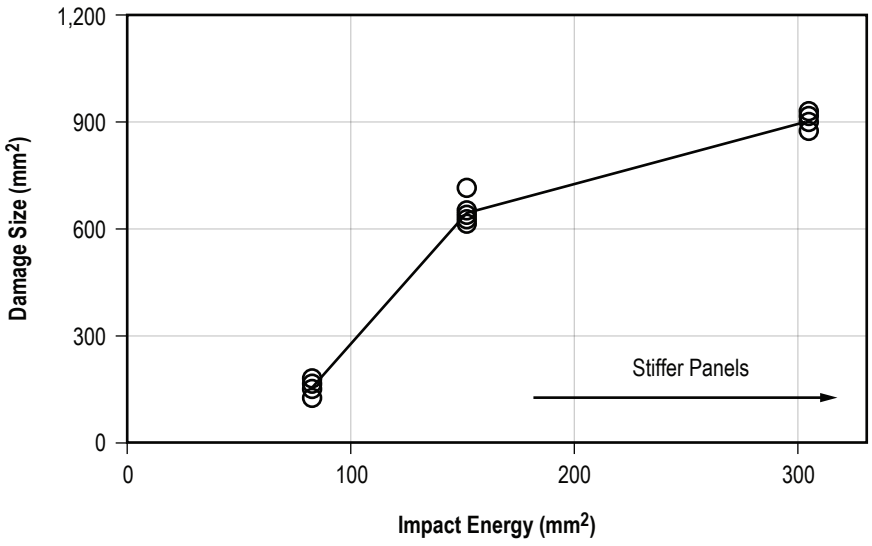

Figure 3. Plot of damage size incurred for a given impact energy as the stiffness of the target increases.[2]

Thus, the size of the panel to undergo CAI testing can be rendered moot if the impact event is accepted as a 'worst case scenario' and all panels rigidly backed. Once damage is inflicted, the next step in a CAI test is to axially load the panel in compression until failure. The CAI strength of three different-sized panels was obtained and presented in reference 2. In addition, some of these panels had a curvature of $r = 1.07$ m to assess if curvature would have any effects on the results. The axial loading on a curved panel is shown in figure 4 for clarity. Results of these tests are shown in figure 5.

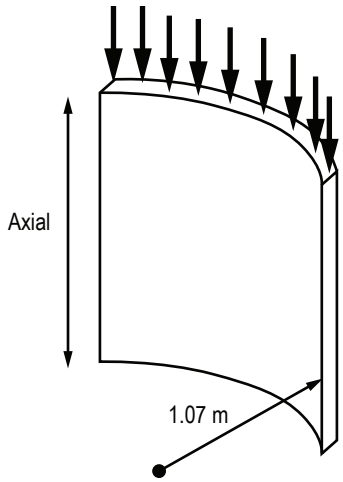

Figure 4. Schematic of loading on subelement curved panels.[2]

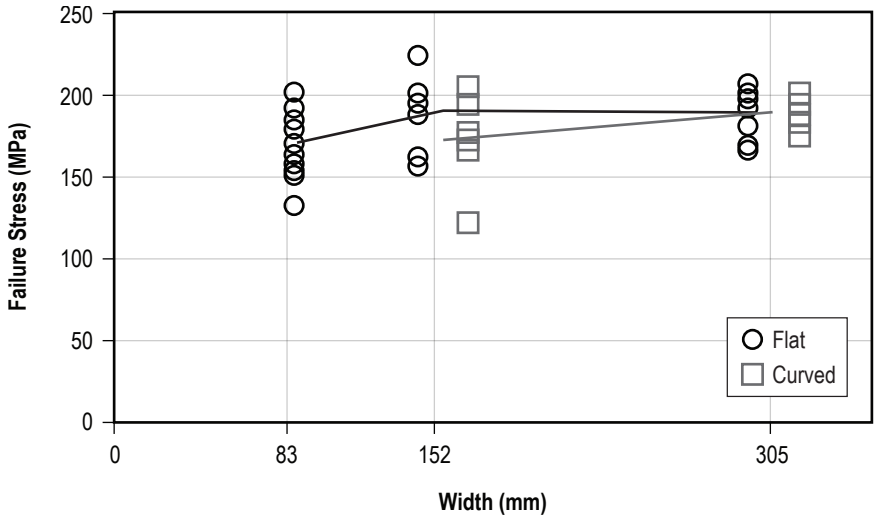

Figure 5. Results of panels tests from reference.[2] Panel width versus CAI failure stress.

One should note that in this study, the wider panels sustained more severe damage since they produced targets that were more rigid than the narrow ones. Despite this, the results show that the smallest panels gave a slightly lower strength than the wider ones. In addition, the curvature of some of the panels had no effect on the resulting CAI strength. Thus if a smaller panel is used to represent a larger one, the results may be conservative, and the larger panels would actually have more load-carrying capability. The lower strength of the narrowest panels was attributed to the interaction of the damage zone with the test panel edges. For the wider panels, the damage zone was sufficiently far away from the edges to cause no detrimental effects. From the conclusion in reference 2, "The global geometry (width and curvature) of specimens larger than a standard size did not affect the damage tolerance of impacted composite sandwich specimens."

In a series of unpublished tests performed by the authors, CAI strength of different-width CAI honeycomb sandwich panels was conducted to assess any size effects. These results are shown in figure 6 and show that no difference could be detected between the wide panels and the smaller ones. The widest panel in the above results may still be considered relatively small compared to a part, such as a 10-m-diameter cylinder. The next section will give physical reasons why larger panels would not be expected to fail at a different load.

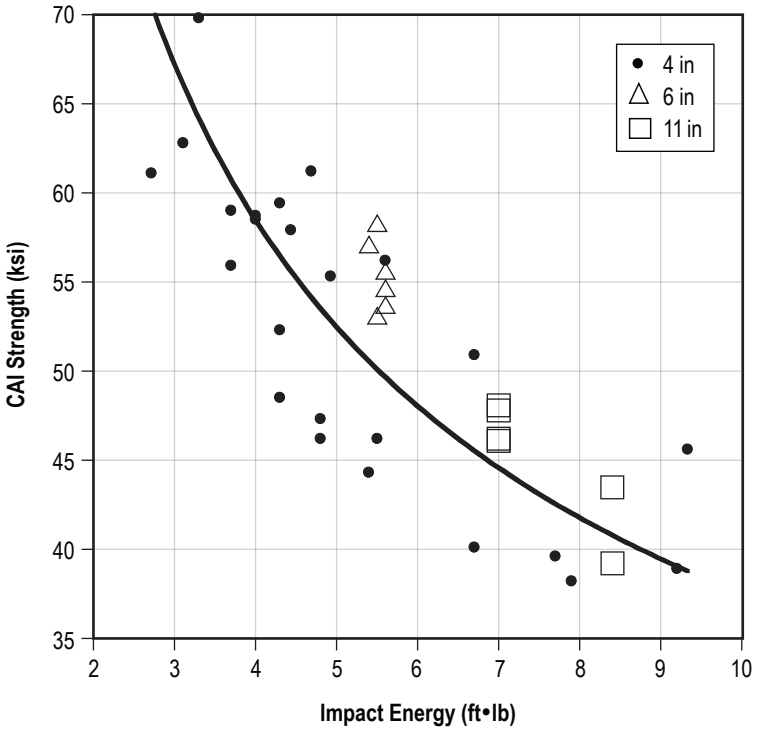

Figure 6. Results of CAI honeycomb panel tests performed by the author (unpublished results).

Since CAI strength is related to damage size in much the same way as open hole compression (OHC) strength is related to hole size (see refs. 3–5), a fiber microbuckling (kink band) mode of failure similar to holes is suggested. The kink band formation/equivalent hole model has been used by others to assess CAI strength of laminates.[6–12] Since impact damage can be represented by holes, examining panel size effects on open hole compression (OHC) tests should give similar results whether the damage in caused by impact or a drilled hole. An expression for hole/edge interaction (finite width correction factor) that has been often used is explained and shown in figure 7. On the left is a wide panel with a hole at the center. This hole will give rise to a stress concentration that raises the stress at the edge of the hole from the applied stress of σ_{app} to a higher value denoted by σ_{hole}. This higher stress, σ_{hole},causes the panel to break sooner than had the hole not been present. For the wide panel on the left, the high stress at the edge of the hole has a chance to decay back to the value of the applied stress σ_{app} before an edge is reached. However for a narrow panel in which the higher stress, σ_{hole} has not decayed back to its global value of σ_{app} before an

edge is reached, the maximum stress (σ_{hole}) will increase even more to accommodate for this. The amount the maximum stress increases due to the edge being close to the hole is given by the finite width correction factor (FWCF) and varies from 1 for wide panels to infinity for the hole being at the edge at the panel edge.

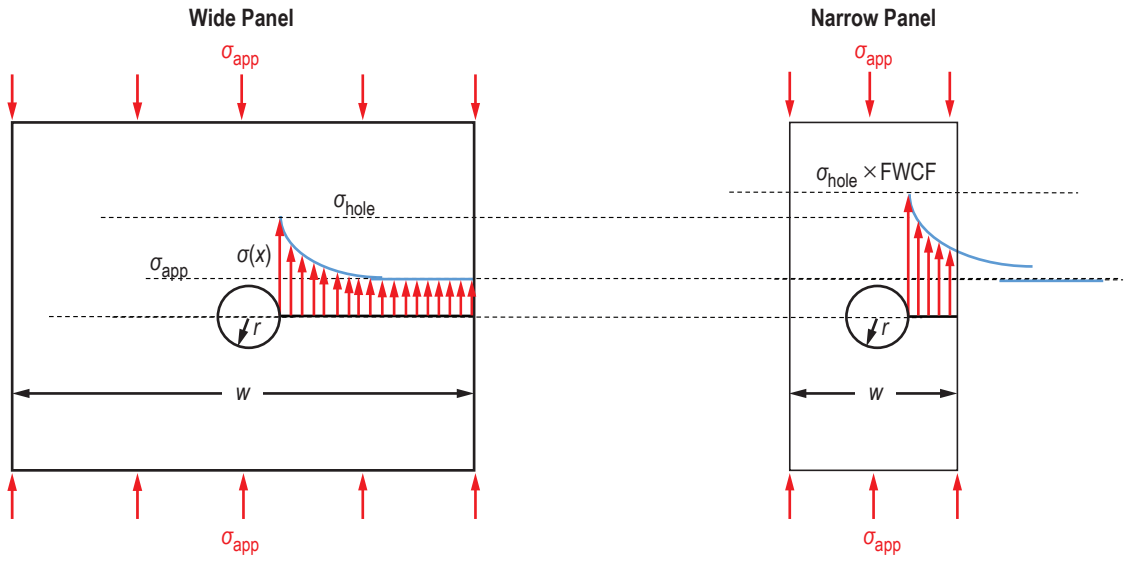

Figure 7. FWCF for holes.[13]

A plot of FWCF as a function of *r*/*w* is shown in figure 8.

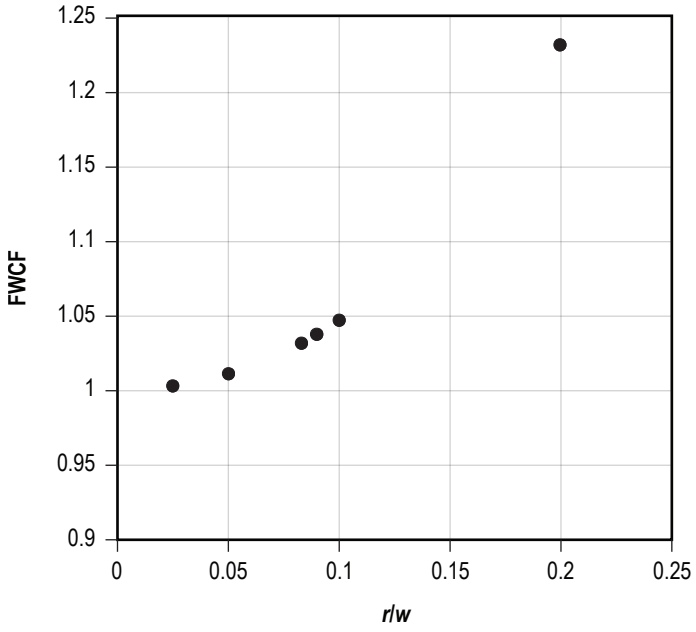

Figure 8. FWCF as a function of *r*/*w*.

When *r*/*w* values are less than 0.025 (hole far from edge), the FWCF is essentially one, thus no correction factor is needed. For a baseline 4-in-wide panel, this equates to a damage size of about 0.2 in. This is a little smaller than what would be expected for a typical BVID for an 8-ply sandwich structure. However, the error is on the side of conservativeness and larger panels would record a higher ultimate stress than the typical 4-in-wide panels. There is no way to decrease the compressive ultimate load carrying capability by increasing the specimen size. Even though a much larger volume of material is being tested, the classical Weibull strength reduction distribution due to small flaws randomly distributed throughout the volume does not apply, as these small flaws are quickly blunted by the carbon fibers (redundant crack stoppers) in the polymer resin. In addition, the induced damage will govern the failure. This damage is a given size, regardless of panel size. This is why coupon level tests (from which allowables are calculated) are accepted being as small since all biases due to small specimen size err on the side of conservativeness. For carbon fiber reinforced polymers, larger-scale structures will demonstrate a higher ultimate stress since the biases due to small specimen geometry (mainly edge effects) are accounted.

In summary, for CAI testing of honeycomb sandwich structure with carbon/polymer facesheets, the width of the specimen is not critical once the width is more than about 10 diameters away from the damage zone. For most impact of the BVID severity, this means a panel width of 20 in or more should have no differences in CAI strength due to size. In addition, any deviations based on smaller panels will give conservative results. In order to maintain a worst-case scenario and negate any effects of panel size on damage formation (not the strength after the damage has been inflicted), it is suggested that all smaller panels be rigidly backed during the impact event.

The preceding information obviously only applies if global panel buckling does not precede the localized failure due to the impact event. Since impact damage is a localized phenomenon, it has no influence on the global stiffness of a sandwich panel. Since the buckling load is dependent upon the global stiffness of the structure, impact damage of the type usually considered (barely visible) is not expected to alter the buckling behavior. The damage would have to be unreasonably large for global stiffness (thus critical buckling load) to be affected. The authors of this Technical Memorandum (TM) wondered if smaller-scale panels could be used to predict the buckling load of larger panels in the same manner that CAI tests could. A recent response from John Hart-Smith, a retired Boeing Technical Fellow and an expert in this field, indicated the following (J.L. Hart-Smith, E-mail Communication, October 15, 2015):

> "The buckling analyses for large structures always involve several wavelengths of the buckling mode in each direction. These intrinsic wavelengths are then a unique function of the w/R ratio for isotropic skins. With small panels, the edge effects count and the buckling stresses are thereby constrained to rise higher.… For a small sandwich panel, this is a very small fraction of a single natural wavelength in each direction, which is totally unrelated to global buckling."

Thus the general consensus appears to be that only a full-scale test can give you the information you need to determine the critical buckling load of a full-scale structure; and the advantages gained by utilizing much smaller specimens, such as can be done for CAI analysis, cannot be done for the buckling mode of failure.

2.1 Using Damage Width to Predict Strength

Of the parameters that can be used to predict the residual compression strength of an impact-damaged sandwich structure, damage width (as detected by either flash thermography of C-Scan) has been found to be the best indicator.[1] An example of an impact-damaged specimen with the width of damage noted is shown in figure 9.

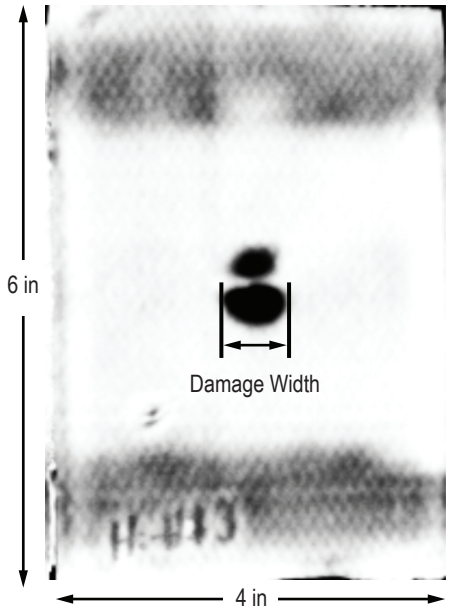

Figure 9. Flash thermography image of impact-damaged sandwich specimen with damage width noted.

2.2 Effect of Impactor Mass

Since a given impact energy can be produced by varying the drop height and mass of an impactor, it was determined that a check of the influence of impactor mass on damage formation should be explored prior to the start of this program. This was motivated by a new impact apparatus that was capable of very low mass impacts, and in the authors' experience, the mass appeared to affect the impact event due to friction with the guide posts—a heavier impactor having more mass to 'overcome" this friction—thus appearing to hit harder for a given impact energy. In a few previous studies,[14,15] the impact mass was found to have little-to-no influence on the type and extent of damage formed in a composite laminate for a given impact energy.

A series of impacts were performed with the mass set at its lowest level (1.1 lb) and its highest height (30.5 in). Then, the impacts were performed at the same energy, but with the heaviest mass the machine could endure (6.6 lb) and the corresponding drop height to give the same impact energy as the light-mass impacts (5 in).

The results showed little difference in maximum load of impact, and no different damage size as ascertained by flash thermography or dent depth. The results are summarized in table 1. Examples of the load/time and load-deflection curves of the two types of impacts are shown in figure 10. The force/displacement traces are similar and, as expected, the duration of the impact for the heavier mass is longer, but of the same magnate as the light mass. This indicates that any noted differences would be due to a time effect (viscoelasticity).

Table 1. Measured responses of 2.5 ft•lb impacts with low and high masses.

Lite Specimen ID	Mass (lb)	Impact Energy (ft•lb)	Maximum Load of Impact	Dent Depth (in)	NDE Width (in)
1	1.1	~2.5*	506	0.023	0.77
2	1.1	~2.5*	495	0.022	0.73
3	1.1	2.49	502	0.023	0.76
4	1.1	2.54	477	0.023	0.77
5	1.1	2.57	488	0.023	0.75
Average		**2.52**	**493.6**	**0.0228**	**0.756**
Standard Deviation		0.04	11.5	0.00045	0.017
Standard Deviation/ Average (%)		1.6	2.3	2	2.2
Heavy Specimen ID	**Mass (lb)**	**Impact Energy (ft•lb)**	**Maximum Load of Impact**	**Dent Depth (in)**	**NDE Width (in)**
1	6.6	2.57	516	0.022	0.74
2	6.6	2.56	513	0.024	0.76
3	6.6	2.37	482	0.022	0.76
4	6.6	2.52	505	0.022	0.76
Average		**2.51**	**504**	**0.0225**	**0.755**
Standard Deviation		0.09	15.4	0.001	0.01
Standard Deviation/ Average (%)		3.6	3.1	4.4	1.3

*Inferred from drop height. Velocity data not obtained.

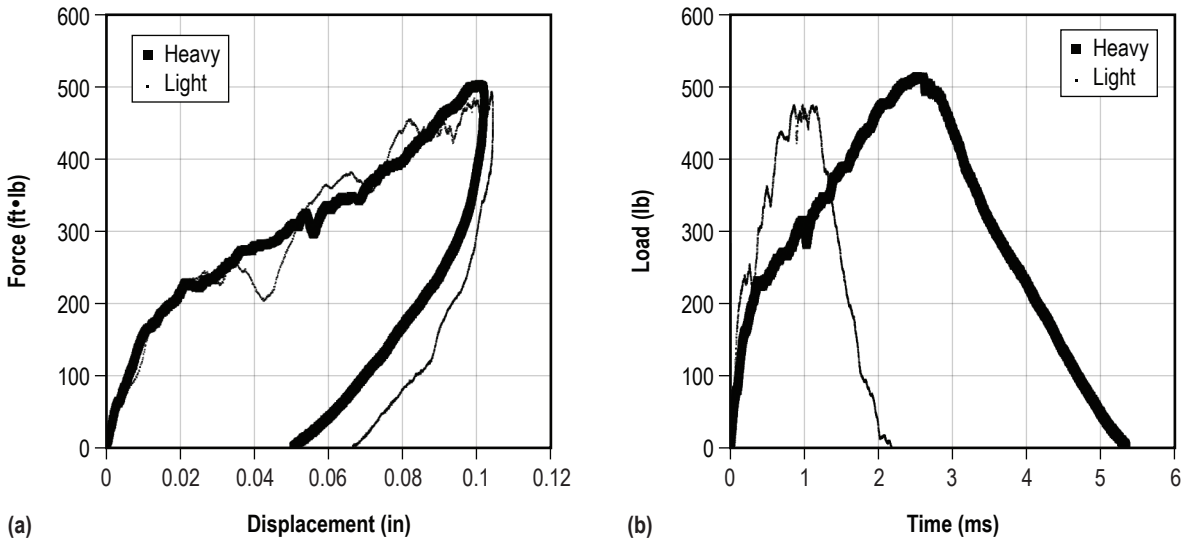

Figure 10. Data for impacts with light and heavy masses: (a) Load-versus-deflection data and (b) load-versus-time data.

As a final check of any differences in the light and heavy mass impacts, the specimens were sectioned through the impact zone, and the through-thickness damage recorded. Upon sectioning, the type and extent of damage did not appear to vary. Examples of the core damage and facesheet damage from each type of impact are given in figure 11. Thus it was concluded that the mass of the impactor was not a variable.

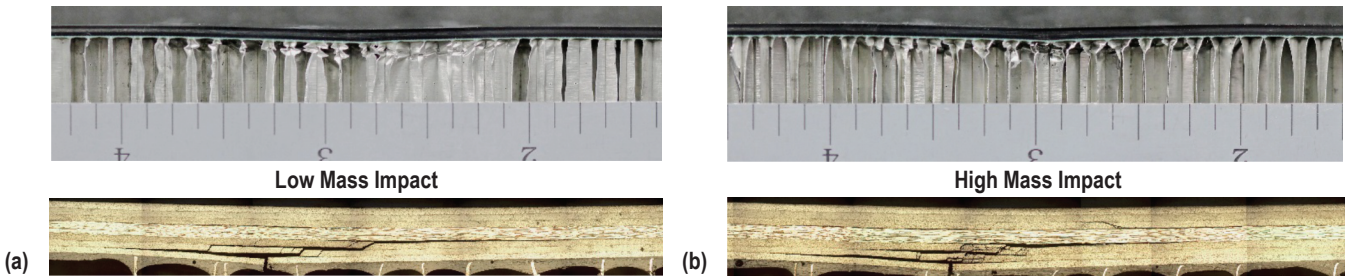

Figure 11. Photographs of core damage (top) and facesheet damage (bottom) for the (a) low-mass impact and (b) high-mass impact.

3. RESULTS OF RISK REDUCTION TESTS ON TYPE I SPECIMENS

During this program, some of the parameters of the sandwich construction were changed; however, all of the results of the risk reduction testing will be presented for completeness. The risk reduction specimens are labeled as type I and type II, as the sandwich structure design changed after a period of time had passed and risk reduction activities were underway. The results are presented in chronological order (i.e., type I first, type II second).

3.1 Undamaged Compression Strength

The undamaged compression strength of the honeycomb sandwich structure can attempt to be measured, but since doing so is very difficult and the results will not be used anyway since damage tolerance concerns must be addressed, these tests will only comprise a small total of the strength tests performed as part of this risk reduction activity. For completeness, the results of limited testing of pristine sandwich structure is presented in table 2.

Table 2. Measured compression strength of undamaged specimens.

Virgin Specimen	Compression Strength (ksi)
1	87.1
2	81.8
3	84.8
4	95.5
5	95.4
6	94
Average	**89.8**
Standard Deviation	5.9

Figure 12 is a schematic of the specimens used in this study. They consisted of 1-in-thick aluminum honeycomb with a density of 3.1 lb/ft^3. The facesheets were made of IM7/8552 carbon/epoxy, and each face was 8-plies with a layup of [+45/0/–45/90]s. The facesheets had a nominal cured thickness of 0.049 in. The 6-in-tall by 4-in-wide specimens were machined from a larger panel that was manufactured by automated tape laying. FM300 film adhesive was placed between the laminate and the core.

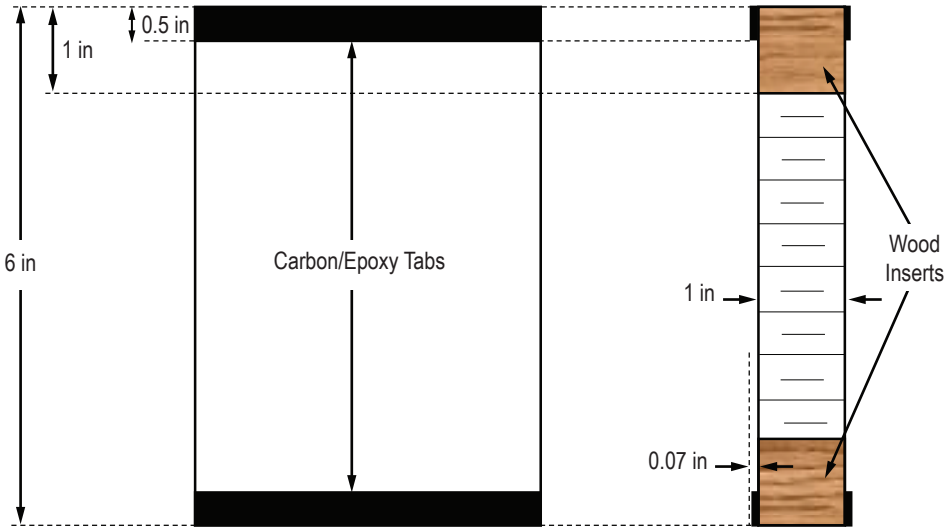

Figure 12. Schematic of specimens used in this study.

In reference 16, specimens made of the same fiber/resin system and layup reported undamaged strengths in the 60–70 ksi range, so the numbers in this study are not considered suspect since they are higher than those found in the other study. The differences in values are probably more a manifestation of different test techniques rather than any differences in material. In fact, although all of the data in table 2 came from the same panel, the first three data points are on the low side, since minor specimen improvements were made, and higher strength values were obtained in the three latter tests. As will be seen, the damaged strength data does not show this type of variability due to testing, since the specimen is being forced to fail at the damage site at a lower load than the undamaged specimens.

3.2 The Effect of Impact Damage

As an upper bound of impact severity, 2.3 ft•lb of energy with a 0.5-in impactor was chosen since this provided visible damage (a dent) that could easily be seen with no special lighting. The CAI results of these tests are given in table 3.

At first glance it appears that there is much 'risk' involved since the compression strength is reduced by 47% over the undamaged specimens shown in table 2; however, as previously mentioned, the undamaged strengths are never used to design load bearing structures, and once damage and other detrimental effects are accounted for, a conservative strain allowable typically used for strength critical carbon fiber composites is 4,000 microstrain. Since the modulus of these sandwich specimens is about 8.6 MSI, the values in table 2 convert to an average strain to failure of 5,600 microstrain. Since the hardware of interest in this study is stiffness critical, the maximum strain the facesheets could experience would be much lower than the typical 4,000 microstrain used in strength critical structure.

Table 3. Measured compression strength of 2.3 ft•lb impact specimens.

Hi Specimen	Impact Energy (ft•lb)	Maximum Load of Impact (lb)	Dent Depth (in)	NDE Width (in)	Compression Strength (ksi)
1	2.3	430	0.0210	0.6	45.9
2	2.31	446	0.0205	0.62	47.2
3	2.39	444	0.0215	0.63	47.2
4	2.43	461	0.0225	0.67	48.4
5	2.35	437	0.0205	0.67	47.8
6	2.32	432	0.0205	0.69	45
7	2.29	426	0.0195	0.67	51.2
Avgerage	**2.34**	**439**	**0.0209**	**0.65**	**47.6**
Standard Deviation	0.052	12	0.00094	0.03	2
Standard Deviation/ Average (%)	2.2	2.7	4.5	4.6	4.2

3.3 The Effect of Core Splices

Since the honeycomb core comes in finite sizes, pieces of it must be joined to manufacture the full-scale structure. This is done by using a 'core splice' adhesive that is essentially a foaming epoxy that bonds the edges of the pieces of honeycomb. Depending on the processing technique and quality, these core splices can have a varying effect on the facesheets as they are laid up and cured on top of these splices. An example of excessive fiber waviness that can result from automated tape laying over a core splice is shown in figure 13. Typically, fiber waviness is to be minimized to maintain the stability of the load-bearing 0º fibers. In order to assure minimal risk, the effects of impacts directly over these core splices were assessed.

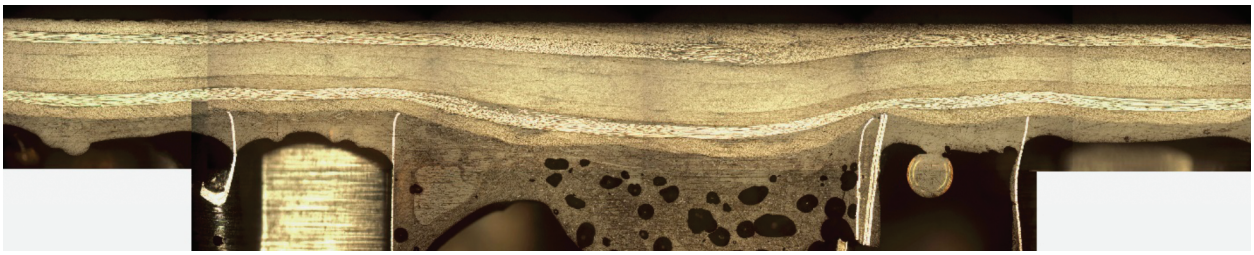

Figure 13. Cross section of fiber waviness caused by core splice adhesive.

Specimens with core splices running horizontally, vertically, or both, to the loading axis were impact damaged right at the core splice (at the intersection of core splices for specimens with both) and subsequently compression tested just as all other specimens were. The results from these tests are summarized in table 4.

Table 4. Summary of impacts over core splices.

Splice Specimen	Splice Orientation	Impact Energy (ft•lb)	Maximum Load of Impact (lb)	Dent Depth (in)	NDE Width (in)	CAI Strength (ksi)
1	Horizontal	2.29	546	0.0135	0.86	36.2
2	Horizontal	2.29	631	0.0110	0.81	35.5
3	Horizontal	2.32	623	0.0115	0.69	42.8
4	Horizontal	2.34	513	0.0105	0.76	51.3
5	Horizontal	2.37	503	0.0110	0.72	45.7
6	Horizontal	2.36	510	0.0120	0.86	38.9
7	Horizontal	2.43	506	0.0135	0.81	50.2
8	Horizontal	2.33	596	0.0105	0.77	51.6
Average		**2.34**	**554**	**0.0117**	**0.79**	**44.1**
Standard Deviation		0.046	55	0.00122	0.062	6.7
Standard Deviation/Average (%)		2	9.9	10.4	7.8	15.2

Splice Specimen	Splice Orientation	Impact Energy (ft•lb)	Maximum Load of Impact (lb)	Dent Depth (in)	NDE Width (in)	CAI Strength (ksi)
9	Vertical	2.25	658	0.0065	0.64	57.7
10	Both	2.31	561	0.0120	0.67	47.1
11	Vertical	2.38	453	0.0215	0.72	42.2
12	Vertical	2.41	453	0.0200	0.70	43
13	Vertical	2.30	522	0.0125	0.72	44.9
14	Both	2.24	805	0.0165	0.59	47.6
Average		**2.32**	**575**	**0.0148**	**0.67**	**47.1**
Standard Deviation		0.068	136	0.0056	0.051	4.83
Standard Deviation/Average (%)		2.9	23.7	37.8	7.6	11.9

A graphic summary of these results with those in table 3 are given in figures 14,15,16 and 17. The results show that the dent depth was smaller and the NDE signature was larger in the direction of the core splice for specimens with the splices as shown in figure 18. The instrumented impact data indicated that the maximum load of impact was higher for impacts over a core splice.

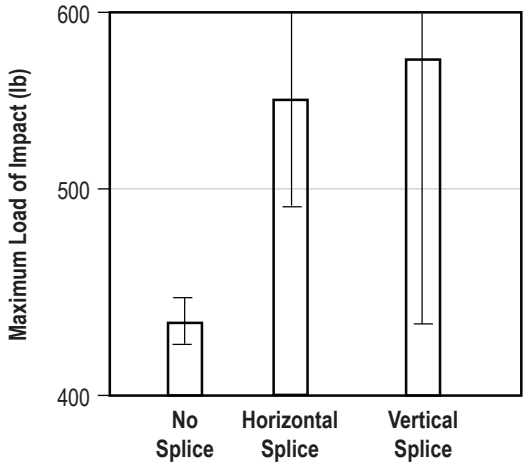

Figure 14. Maximum load of impact data for specimens with and without core splices impacted at 2.3 ft•lb of impact energy.

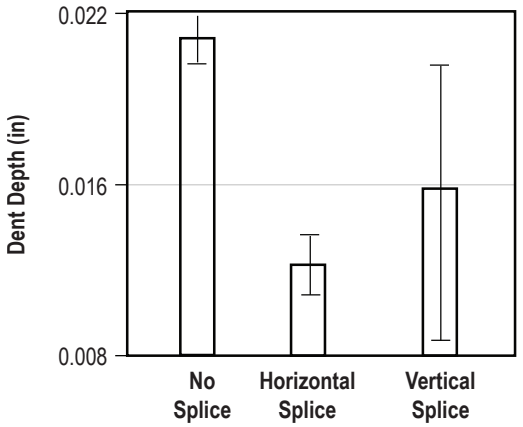

Figure 15. Dent depth data for specimens with and without core splices impacted at 2.3 ft•lb of impact energy.

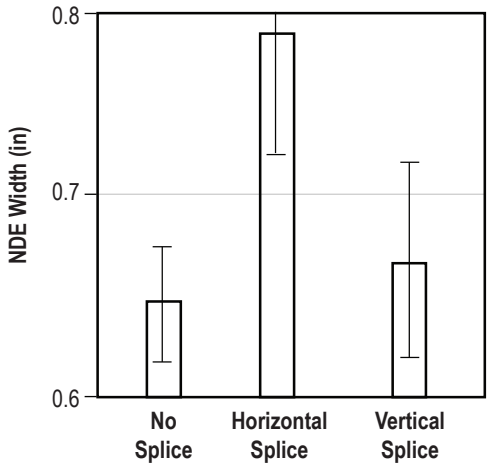

Figure 16. NDE width data for specimens with and without core splices impacted at 2.3 ft•lb of impact energy.

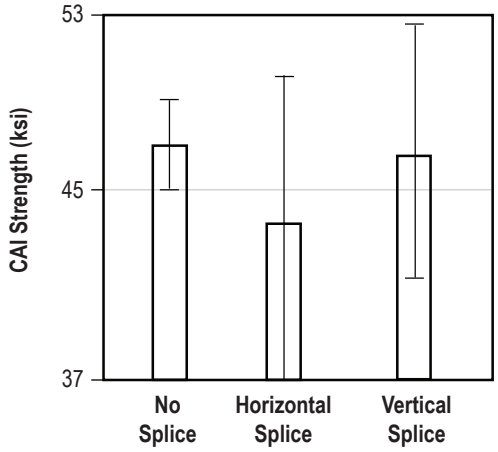

Figure 17. CAI strength data for specimens with and without core splices impacted at 2.3 ft•lb of impact energy.

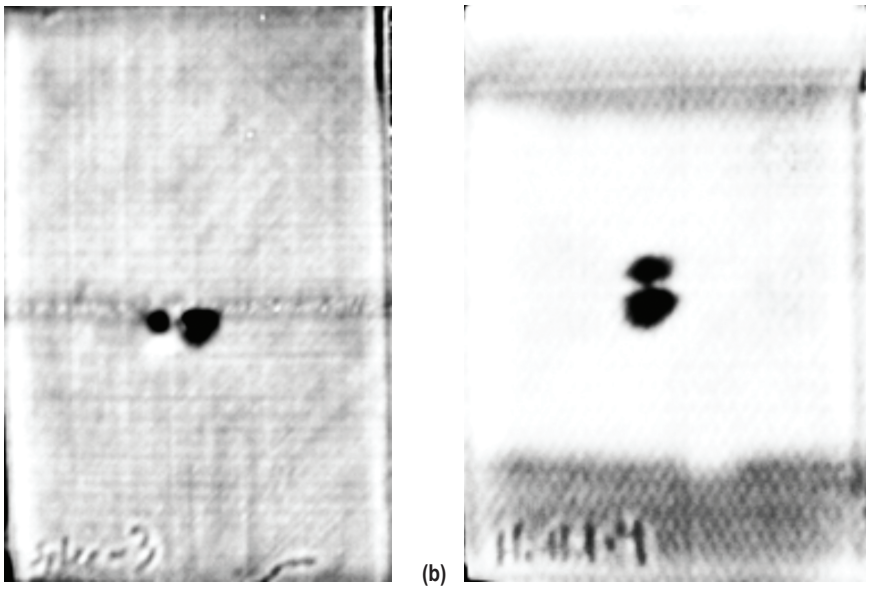

Figure 18. Flash thermography indications of 2.3 ft•lb impacts: (a) Over a core splice and (b) not over a core splice.

The compression tests showed that the vertical splices had no detrimental effect on compression strength, but the horizontal splices failed lower than similarly impacted specimens with no core splice. This is not surprising, given that the damage width as measured by NDE was wider for the horizontal splices and, as stated earlier, damage width appears to be the governing factor in determining CAI strength. The core splice specimens showed large amounts of scatter in CAI strength compared to those specimens with no core splice.

A visual comparison of specimens with and without a core splice impacted at 2.3 ft•lb is shown in figure 19. Although the impact not over the core splice measures an overall deeper depth, the impact over the core splice is more localized (overall dent not as wide and more gradual) and is thus actually easier to see.

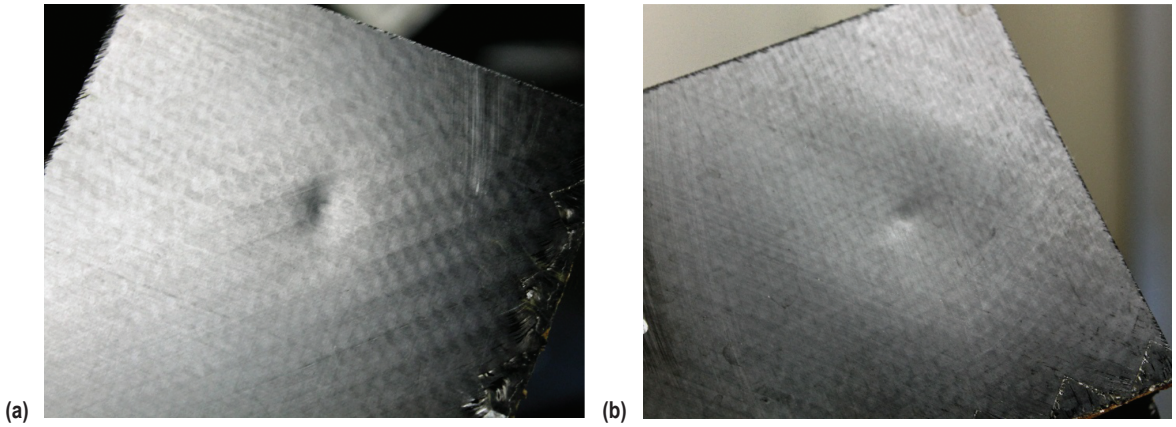

Figure 19. Visual comparison of 2.36 ft•lb impacts: (a) Over a core splice and (b) not over a core splice.

Cross-sectional views of the dents shown in figure 19 are shown in figure 20. Note that there is more core crushing in the specimen with no splice. A closer examination of the damage in the facesheets are shown in figure 21.

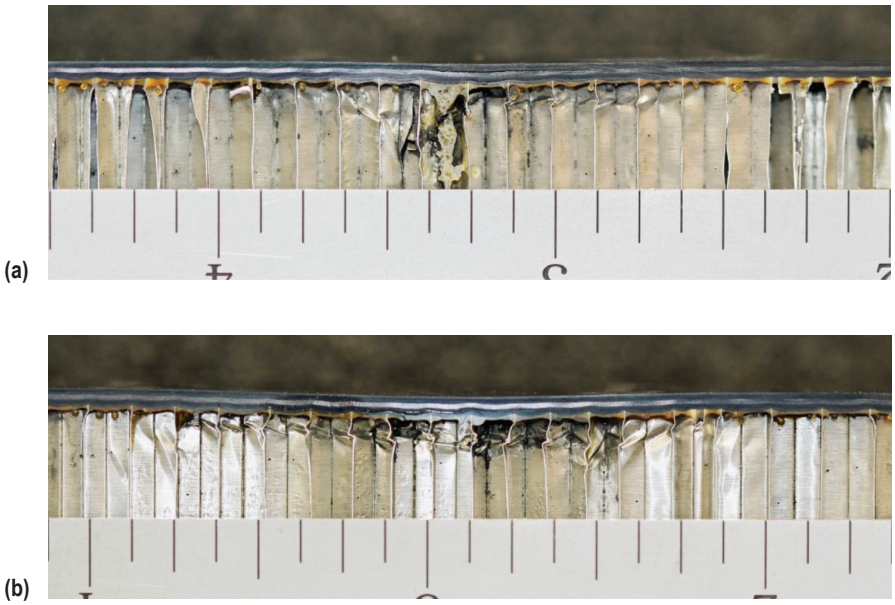

Figure 20. Cross sections of dents due to 2.3 ft•lb impacts in specimens: (a) With a core splice and (b) without core splice.

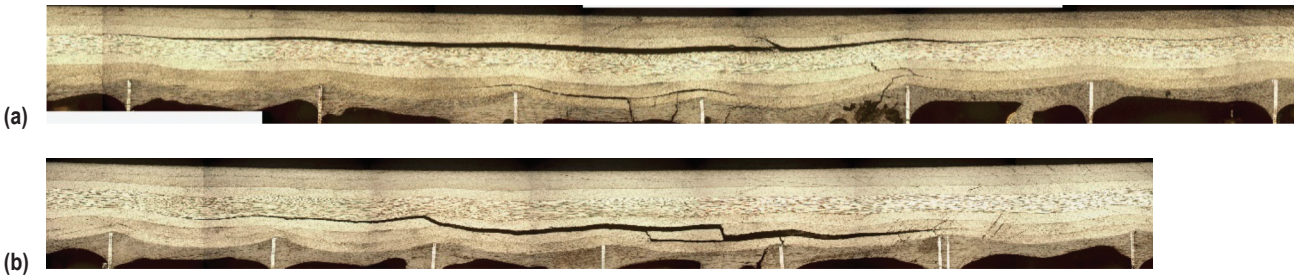

Figure 21. Damage in facesheets of the two specimens in figure 20: (a) Over core splice and (b) no core splice.

Specimens with horizontal core splices without impact damage were also tested to see if the undamaged strength was lowered due to the core splices. One specimen did break along the core splice at a relatively low value, but this value was still well above whatever impact damaged compression strength to which the structure would be designed; thus the most critical area for impact damage in the acreage of the Type I structure is on top of a core splice that is oriented horizontally to the compressive load. The dent depth is lessened, but visual identification is the same. The residual compression strength is lowered.

3.4 The Effect of Holes

Many composite structures are sized based on the strength of the laminate with a hole in it. Typically, the hole size is taken to be 0.25-in diameter. This OHC strength is usually the design driver. As a check against the CAI data generated, sandwich specimens were compression tested with a 0.25-in hole at the center rather than impact damage. The results are summarized in table 5.

Table 5. OHC results of sandwich specimens.

Hole Specimen	Compression Strength (ksi)
1	41.6
2	40.1
3	43
4	44.3
5	48.1
6	44.5
7	42.3
Average	**43.5**
Standard Deviation	2.6
Standard Deviation/Average (%)	5.9

These results show that the CAI strength (47.6 ksi) is, on average, slightly higher than the OHC strength (43.5 ksi) and about the same as specimens with a horizontal core splice impacted at 2.3 ft•lb of energy (44.1 ksi). Thus 0.25-in holes and BVID over the worst acreage location (horizontal core splices) give similar strength values in these specimens.

3.5 The Effect of Foreign Object Debris

Other than impact damage, another type of damage that may possibly occur to the structure is the presence of foreign object debris (FOD) within the laminate during processing. The most common example of this is a piece of release film or Teflon tape finding its way into the structure during processing. A real-world example of this occurred on the X-33 liquid hydrogen tank, which failed partly due to the existence of FOD between the facesheet and core. With this in mind, a series of tests were conducted to assess the compression strength of sandwich structure with FOD between the facesheet and core. The results are shown in table 6. The FOD was represented by square pieces of Teflon either 1 or 2 in on a side as shown in figures 22 and 23. Three replicates were fabricated with 1-in square sections of FOD, and three replicates were fabricated with 2-in square sections of FOD.

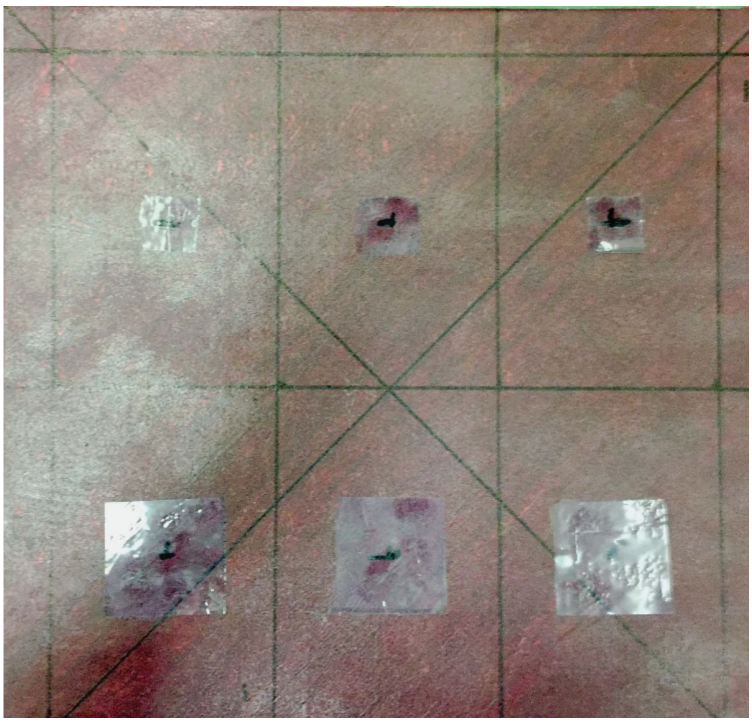

Figure 22. Photograph of square pieces of Teflon™ (FOD) placed on facesheet before bonding to the core.

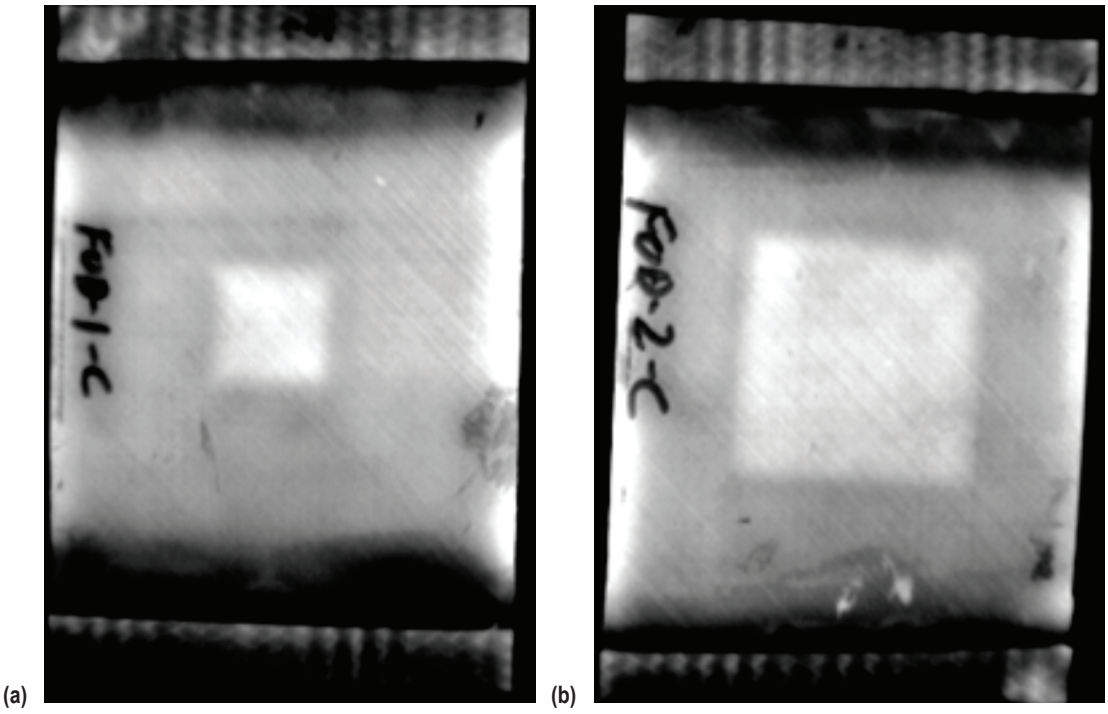

Figure 23. Flash thermography of square pieces of Teflon FOD placed between facesheet and core: (a) 1-in square and (b) 2-in square.

Table 6. Compression results of sandwich specimens with FOD between facesheet and core.

FOD Specimen	FOD Size (in)	Compression Strength (ksi)	Notes
1-A	1×1	51.4	Broke on non-FOD side
1-B	1×1	42.3	Broke due to fiber fracture at bottom of FOD
1-C	1×1	50.9	Broke away from FOD
2-A	2×2	34.1	Broke at FOD
2-B	2×2	50.5	Broke on non-FOD side
2-C	2×2	54.7	Broke at FOD. Facesheet did not separate from core.

It can be seen that for all but one of the specimens with the two-inch square FOD the values are above those obtained for holes. Since the lower bound of FOD is typically set at 1-in in planar dimension, the 2-in square FOD is not realistic and would never pass inspection. Thus FOD that may go undetected by NDE will not be detrimental to the compression strength of the sandwich structure.

4. TYPE II SPECIMENS

A change in core density and facesheet layup was called for by the program. These specimens (called type II in this report) needed to be tested for damage tolerance to ascertain any differences due to these small changes. The changes were as follows:

- Core density increased from 3.1 to 4.4 lb/ft^3.
- Facesheet layup changed from [45/0/–45/90]S to [45/90/–45/0]s.
- An adhesive paste, rather than a foaming film adhesive, was used to splice core.
- Other than these two changes, all other parameters remained the same.

4.1 Definition of Barely Visible Impact Damage

The impact energy that caused BVID on the first type of panels was used to impact the new type of sandwich structure. The dent depths were smaller for the new specimens due to the higher density core; however, the damage was still visible as shown in figure 24.

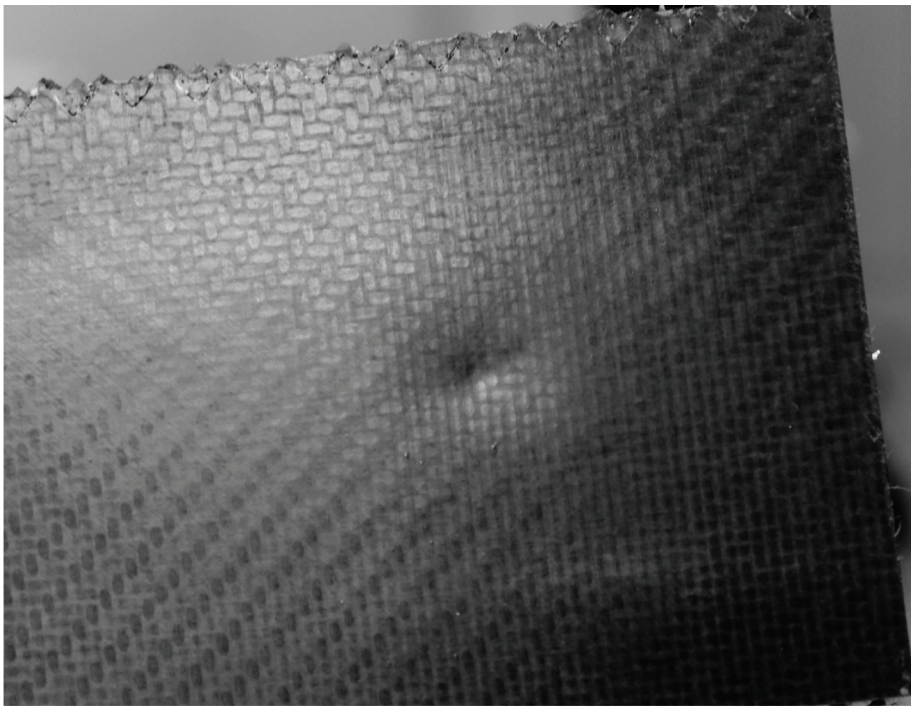

Figure 24. Visual damage to facesheet of type II sandwich structure impacted at 2.3 ft•lb of energy.

4.2 The Effect of Impact Damage

As an upper bound of impact severity, 2.3 ft•lb of energy with a 0.5-in impactor was chosen, since this provided visible damage (a dent) that could easily be seen with no special lighting. The CAI results of these tests are given in table 7.

Table 7. Measured compression strength of type II impact specimens.

Type II Specimen	Impact Energy (ft•lb)	Maximum Load of Impact (lb)	Dent Depth (in)	NDE Width (in)	Compression Strength (ksi)
1	No data	No data	0.0115	1.01	52
2	2.36	524	0.0110	1.01	51.7
3	2.4	537	0.0140	1.01	51.4
4	2.41	505	0.0100	1	49
5	2.24	498	0.0120	0.97	53.9
6	2.24	514	0.0130	1.03	No data
7	2.22	500	0.0140	1.01	53.6
8	2.22	482	0.0115	1	58.9
Average	**2.3**	**509**	**0.0121**	**1.01**	**52.9**
Standard Deviation	0.087	18	0.0014	0.017	3.1
Standard Deviation/Average (%)	3.7	3.5	11.6	1.7	5.9

The average maximum load of impact is higher and the dent depth lower than the type I specimens as expected due to the higher density core. The damage area as detected by flash thermography is also larger.

A cross-sectional view of the damage formed from a 2.3 ft•lb impact on a type II specimen is shown at the bottom of figure 25, and a similar view from a 2.3 ft•lb impact on a type I specimen is shown at the top of the figure. The larger damage areas as detected by NDE is evident as there is more damage through the thickness of the specimen.

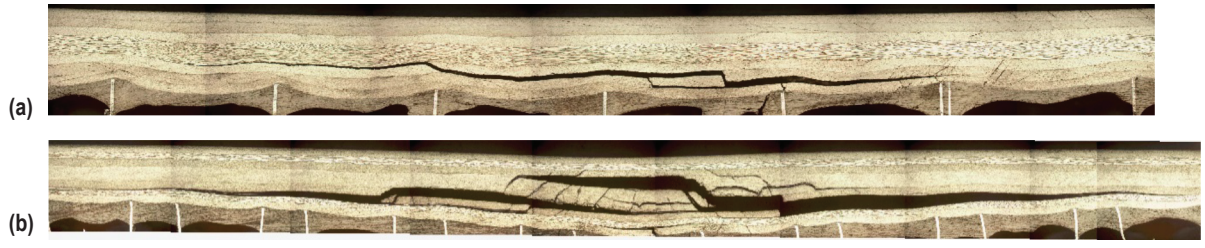

Figure 25. Cross-sectional views of impact damage to (a) type I specimen and (b) type II specimen.

The average CAI strength is seen to be slightly higher for these specimens than the type I specimens (45.6 ksi versus 41.0 ksi) despite the NDE width being larger for the type II specimens. This result was not fully expected, and rationalization as to the mechanisms of this needs to be explored further for a definitive explanation; however, for the practical implications, this is a good result as larger NDE areas are easier to detect. If easier detection can occur without a loss in compression strength, then this is a positive, regardless of the reasons why.

4.3 The Effect of Core Splices

The newer type II specimens had core spliced together by injecting a paste epoxy into the gap between core sections rather than by a foaming film adhesive as was done with the first set of sandwich specimens. Photographs of the two types of core splices (in the 90° direction) are shown in figure 26. Figure 13 shows the 0° ply waviness that occurs in the foam adhesive type splice. Figure 27 shows the improved straightness of the fibers over the paste adhesive type splice. Since the type I specimens demonstrated a lower CAI strength when the impact was directly over a horizontal core splice, some CAI tests were performed on the new type of core splice. Table 8 summarizes impacts over the new core splice.

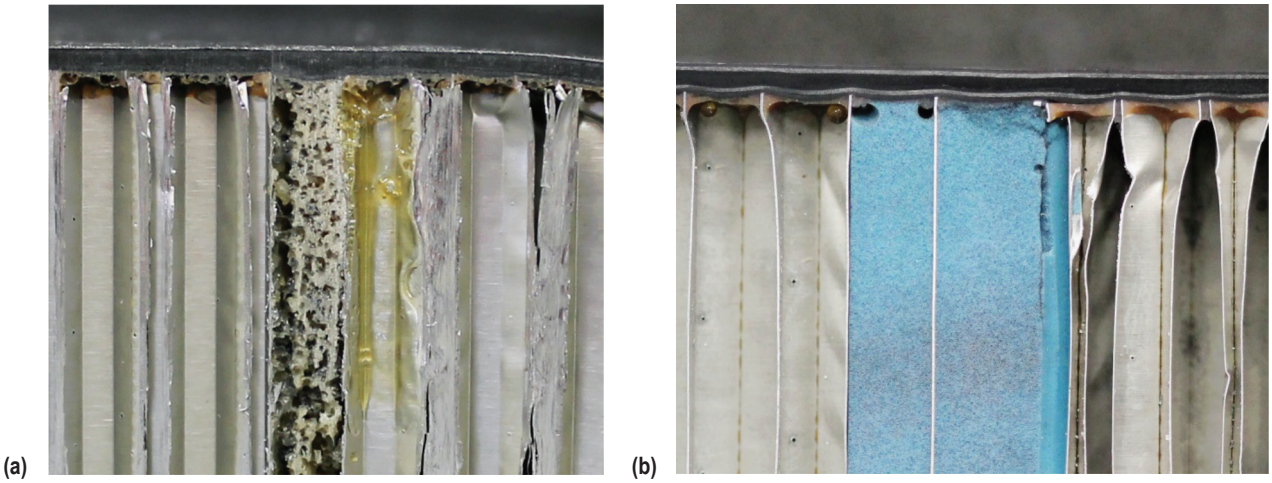

Figure 26. Two types of core splices: (a) Foaming adhesive splice and (b) past adhesive splice.

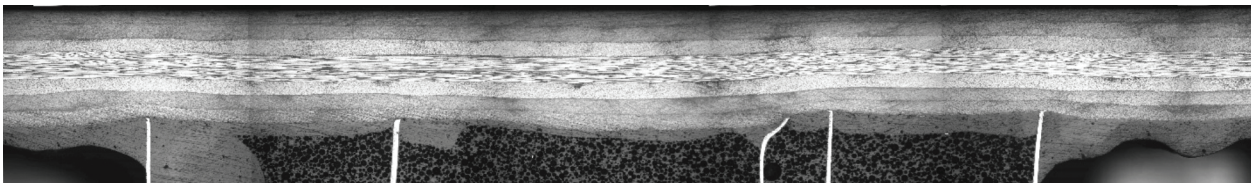

Figure 27. Improved 0° fiber waviness over paste adhesive type splice.

Table 8. Summary of impacts over new core splices.

Splice Specimen	Splice Orientation	Impact Energy (ft•lb)	Maximum Load of Impact (lb)	Dent Depth (in)	NDE Width (in)	CAI Strength (ksi)
1	Horizontal	2.28	888	0.0045	0.53	68.8
2	Horizontal	2.23	750	0.0061	0.71	56.5
3	Horizontal	2.26	734	0.0050	0.58	63.2
4	Horizontal	2.24	737	0.0030	0.58	59.4
Average		**2.26**	**777**	**0.0047**	**0.6**	**62**
Standard Deviation		0.022	74	0.0013	0.08	5.3
Standard Deviation/Average (%)		1	9.5	2.8	13	8.5

In contrast to the type I specimens, impacts over horizontal core splices are not as detrimental as a similar impact within the acreage. Thus, the most critical area for impact damage in the acreage of the Type II structure is away from a core splice. The dent depth is lessened due to the core splice, and this results in a smaller damage sie and higher CAI strength.

4.4 Specimens With Outer Ply of Cloth

As part of this program, the feasibility of adding an outer layer of woven carbon cloth prepreg to aid in damage tolerance and fiber breakout during drilling operations was assessed. These were type II specimens, with the only difference being a ply of SGP370-8H/8552 8-harness satin weave cloth being placed on both the bag and the tool side of the sandwich structure. This added a thickness of 0.02 in to each facesheet, resulting in a total thickness of 0.067 in for each facesheet. This results in an approximate addition of weight of 18% over noncloth-covered honeycomb sandwich structure.

Since the facesheets are now thicker, the energy needed to create BVID had to be determined. It was assumed that this energy would be greater than the 2.3 ft•lb needed for the noncloth-covered sandwich structure. Figure 28 shows some trial hits on sections of cloth covered sandwich structure.

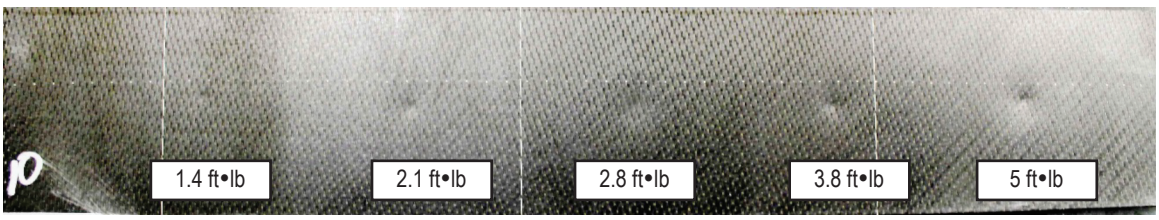

Figure 28. Impact trials on cloth-covered honeycomb sandwich structure.

A general consensus was that close to 3.8 ft•lb impact was readily visible. This represented a 54% increase in impact energy needed for BVID over the noncloth-covered honeycomb sandwich structure. However, since the facesheets are thicker, they may handle this increased impact energy such that the CAI strengths of the cloth- and noncloth-covered sandwich structure would be similar. Table 9 shows the results of CAI testing on cloth-covered honeycomb sandwich structure.

Table 9. Measured CAI strength of type II specimens with cloth layer.

Cloth Specimen	Impact Energy (ft•lb)	Maximum Load of Impact (lb)	Dent Depth (in)	NDE Width (in)	Compression Strength (ksi)
1	3.65	687	0.0105	1.05	49
2	3.67	691	0.011	1.22	41.4
3	3.7	739	0.011	1.17	48.9
4	3.66	726	0.0105	1.16	45.5
5	3.67	692	0.0135	1.15	40.3
6	3.7	703	0.011	1.16	41.5
7	3.67	713	0.0105	1.07	50.1
8	3.69	713	0.012	1.06	45.2
Average	**3.68**	**708**	**0.0113**	**1.13**	**45.2**
Standard Deviation	0.02	18	0.001	0.06	3.9
Standard Deviation/ Average (%)	0.5	2.5	8.8	5.3	8.6

These results show that the CAI strength is lower than the noncloth-covered type II specimens; thus there must be compelling evidence that the outer layers of cloth are needed to justify the 18% weight increase and 15% BVID CAI strength reduction.

5. REPAIR

Since any damage will need to be repaired, damage was introduced into sandwich specimens and repairs were made to assess how much of the original strength could be regained. For thin facesheet honeycomb structure, scarf repairs are generally not feasible and patch repairs are typically used.[17–19]

The first repairs were done on specimens with holes since misdrilled holes are not an uncommon occurrence. Simple patch repairs consisting of 8 plies of IM7/5320-1 out-of-autoclave (OoA) carbon/epoxy were used for the repairs. The holes were first filled with epoxy resin to prevent the patches from draping into the hole during cure once the holes were filled with epoxy and the epoxy cured. The surface of the specimens to which the repair was to be bonded was prepared by abrading until the outermost fibers in the top layer was visible. Preliminary testing on similar samples demonstrated that a more aggressive surface preparation kept the patches from popping off during compression testing. The patches had the same layup as the parent laminate [45/90/–45/0]s. FM 300 film adhesive was used between the patches and the specimens to aid in adhesion. The plies of the patches were made successively smaller by 0.25 in per ply to minimize edge effects. The patches were circular with an outermost diameter of 3.5 in (innermost diameter of 2 in). The patches were applied with the smaller plies close to the specimen (‘reverse wedding cake’) and with the larger plies next to the film adhesive (‘wedding cake’). Schematics of these repairs are shown in figures 29 and 30. A front view photograph of a repaired specimen in shown in figure 31.

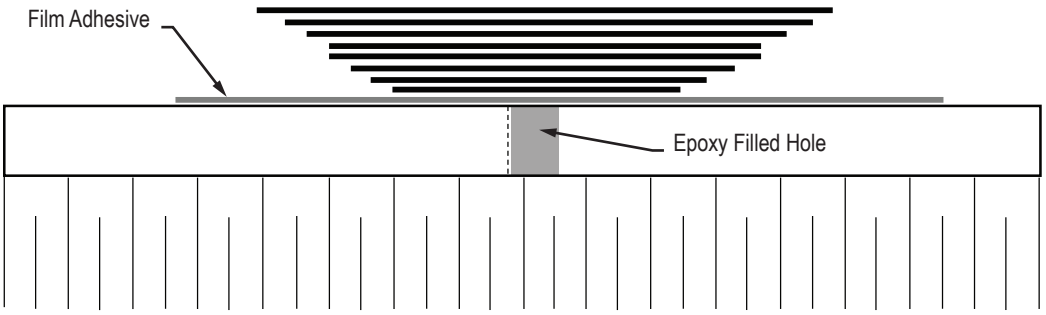

Figure 29. Schematic of reverse wedding cake repair.

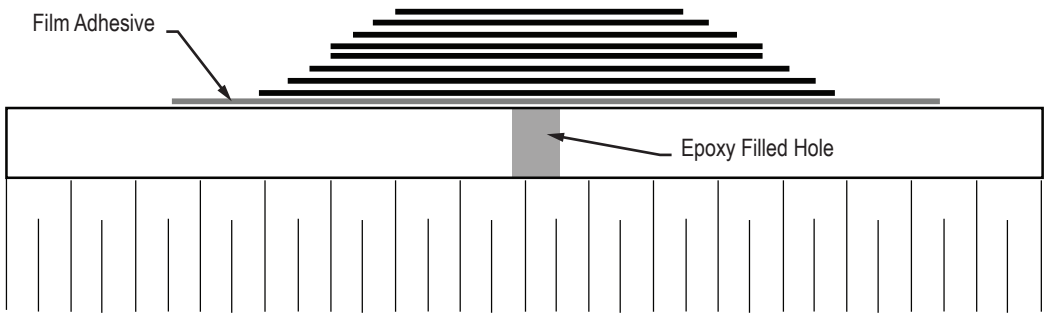

Figure 30. Schematic of wedding cake repair.

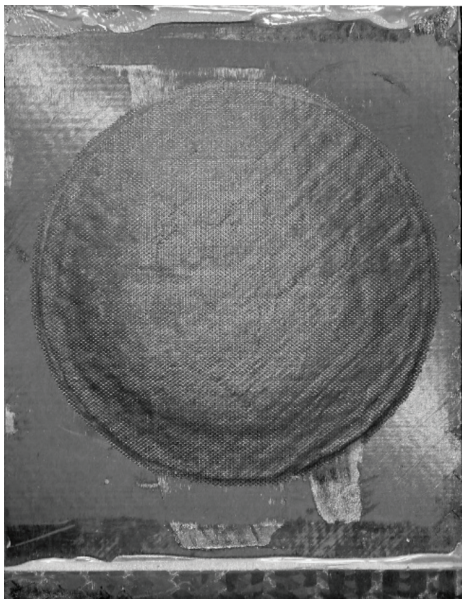

Figure 31. Photograph of repaired specimen.

Subsequent compression testing of these specimens gave strength results of 80.9 and 82.1 ksi for the reverse wedding cake and wedding cake samples, respectively. The failure zone of the wedding cake repair was near the original hole, and the failure location of the reverse wedding cake sample was away from the repair. However, the strength values demonstrated that about 94% of the undamaged strength (≈90 ksi) was recovered.

Since time and material were limited, repairs of impact damage where attempted next, despite the limited number of repaired hole specimens. Specimens were impacted with about 2.4 ft•lb of energy. Earlier results of this severity of impact are presented in table 7. The reverse wedding cake method was decided upon to repair these specimens, since this is typical industry practice. At first, the film adhesive and patches were applied to the impact-damaged laminate

without removing or filling the damage zone. Two specimens were tested in this manner, and the results gave compression strengths of 66.8 and 58.2 ksi, an improvement over the impact-damaged, nonrepaired average strength of 52.9 ksi, but not up to the strength obtained from the repaired holes. The failure location was on the nonimpacted side of the specimens, indicating that the repair was not carrying the amount of load it should (I.e., it was 'soft' and dumped excess load onto the undamaged facesheet.) since the impact damage causes a dent in the specimen. It was suspected that the patch conformed to this dent during cure, thus the 0° load bearing fibers were not as straight as desired, so they had a lower modulus.

The next set of specimens had the dent filled smooth with epoxy resin before applying the film adhesive and patch. A photograph of an impacted specimen with the dent filled flush to the surface with epoxy is shown in figure 32. Table 10 lists the results of the compression strength of these repaired specimens.

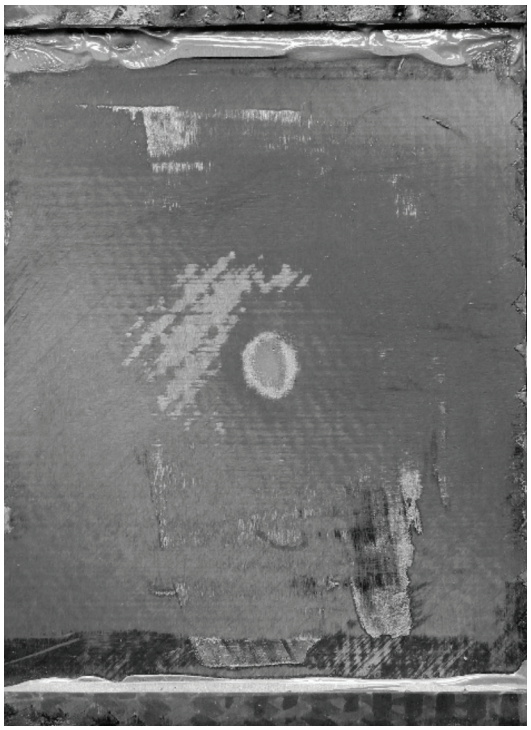

Figure 32. Photograph of impact dent filled and smoothed with epoxy.

Table 10. CAI results of patch-repaired specimens.

Repair Specimen	Impact Energy (ft•lb)	Maximum Load of Impact (lb)	Dent Depth (in)	NDE Width (in)	CAI Strength (ksi)	Region of Failure
3	2.47	522	0.009	0.89	76.3	End broom
4	2.46	585	0.0155	0.71	82.1	Bottom between tab and repair
5	2.48	612	0.015	1.01	87.2	Bottom between tab and repair
6	2.45	628	0.011	0.97	81.5	Broke at repair
7	2.45	610	0.013	0.97	77.5	End broom
8	2.45	624	0.014	1.01	85.4	Broke at repair
9	2.43	583	0.015	1	90.5	Bottom between tab and repair
Average	**2.46**	**595**	**0.0132**	**0.94**	**82.9**	
Standard Deviation	–	–	–	–	5.1	

Thus on average, about 92% of the undamaged strength (89.8 ksi) was recovered. This compares similarly to other studies that have used various methods to repair impact damaged honeycomb structure.[18–21] More detailed studies into repair will be conducted as a follow-on to this effort, including repair of more severe damage. However, at this point, it is evident that a simple patch repair will work for small damages within the acreage of the honeycomb structure.

REFERENCES

1. Nettles, A.T.; and Jackson, J.R.: "Developing a Material Strength Design Value Based on Compression After Impact Damage for the Ares I Composite Interstage," NASA/TP-2009-215634, NASA Marshall Space Flight Center, Huntsville, AL, 52 pp., January 2009.

2. Moody, R.C.; and Vizzini, A.J.: "Test and Analysis of Composite Sandwich Panels With Impact Damage," DOT/FAA/AR-01/124, U.S. Department of Transportation, Federal Aviation Administration, Springfield, VA, May 2002.

3. Soutis, C.; Smith, F.C.; and Matthews, F.L.: "Predicting the compressive engineering performance of carbon fiber-reinforced plastics," *Composites: Part A*, Vol. 31, No. 6, pp. 531–536, June 2000.

4. Guild, F.J.; Hogg, P.J.; and Prichard, J.C.: "A model for the reduction in compression strength of continuous fibre composites after impact damage," *Composites*, Vol. 24, No. 4, pp. 333–339, June 1993.

5. Soutis, C.; and Curtis, P.T.: "Prediction of the post-impact compressive vstrength of cfrp laminated composites," *Compos. Sci. Technol.*, Vol. 56, No. 6, pp. 677–684, doi: 10.1016/0266-3538(96)00050-4, 1996.

6. Chen P.; Shen Z.; and Wang J.: "A New Method for Compression After Impact Strength Prediction of Composite Laminates," *J. Compos. Mater.*, Vol. 36, pp. 589–610, March 2002.

7. Bull, D.J.; Spearing, S.M.; and Sinclair, I.: "Quasi-static indentation and compression after impact damage growth monitoring using microfocus X-Ray computed tomography," in *Proceedings 19th International Conference on Composite Materials*, ICCM, Montreal, CA, 9 pp., 2013.

8. Rivallant, S.; Bouvet, C.; Abdallah, E.A.; Broll, B.; and Barrau, J-J.: "Experimental analysis of CFRP laminates subjected to compression after impact: The role of impact-induced cracks in failure," *Compos. Struct.*, Vol. 111, pp. 147–157.

9. Edgren, F.; Asp, L.E.; and Bull, P.H.: Compressive failure of impacted NCF composite sandwich panels- Characterization of the failure process," *J. Compos. Mater.*, Vol. 38, No. 6, pp. 495–514, 2004.

10. Czabaj, M.W.; Zehnder, A.T.; Davidson, B.D.; and Singh, A.K.: "Compressive strength of honeycomb-stiffened graphite/epoxy sandwich panels with barely-visible indentation damage," *J. Compos. Mater.*, Vol. 48, No. 20, pp. 2455–2471, August 2013.

11. Edgren, F.; Soutis, C.; and Asp, L.E.: "Damage tolerance analysis of NCF composite sandwich panels," *Compos. Sci. Technol.*, Vol. 68, No. 13, doi: 10.1016/j.compscitech.2008.04.041, pp. 2635–2645, October 2008.

12. Lee, J.; Soutis, C.; and Kong, C.: "Prediction of compression-after-impact (CAI) Strength of CFRP Laminated Composites," in *Proc. 18th International Conference on Composite Materials*, ICCM, Jeju, Korea, 9 pp., 2011.

13. Jones, R.M.: *Mechanics of Composite Materials*, 2nd ed., Taylor & Francis, Inc., Washington, D.C., 546 pp., 1998.

14. Ambur, D.R.; and Kemmerly, H.L.: "Influence of Impactor Mass on the Damage Characteristics and Failure Strength of Laminated Composite Plates," Paper Presented at 39th AIAA/ASME/ASCE/AHS/ASC Structures, Structural Dynamics, and Materials Conference, Long Beach, CA, April 20–23, 1998.

15. Artero-Guerro, J.A.; Pernas-Sánchez, J.; López-Puente, J.; Varas, D.: "Experimental study of the impactor mass effect on the low velocity impact of carbon/epoxy woven laminates," *Compos. Struct*., Vol. 133, No. 1, pp. 774–781, 2015.

16. Czabaj, M.W.; Zehnder, A.T.; Davidson, B.D.; et al.: "Compressive Strength of Honeycomb-Stiffened Graphite/Epoxy Sandwich Panels with Barely-Visible Indentation Damage," *J. of Compos. Mater.*, Vol. 48, No. 20, pp. 2455–2471, August 2013.

17. Dutton, S.; Kelly, D.; Baker, A.A.: *Composite Materials for Aircraft Structures, Second Edition*, AIAA, Reston, VA, 400 pp., 2004.

18. Raju, M.; Rajasekhar, R.; Swamy, M.R.; et.al.: "Repair Effectiveness Studies on Impact Damaged Sandwich Composite Constructions," *J. Reinf. Plast. Comp.*, Vol. 25, No. 1, pp. 5–10, January 2006.

19. Park, H.: "Investigation on repairable damage tolerance for structural design of aircraft composite structure," *J. Compos. Mater.*, doi: 10.1177/0021998316643579, April 2016.

20. Mahdi, S.; Kinloch, J.; Matthews, F.L.; and Crisfeld, M.A.: "The Static Mechanical Performance of Repaired Composite Sandwich Beams: Part I - Experimental Characterization," *J. Sandw. Struct. Mater.*, Vol. 5, No. 2, pp. 179–202, April 2013.

21. Cox, S.: "Composite Structures Repair Development at Kennedy Space Center," Paper Presented at LSU College of Engineering Sidney E. Fuchs Seminar Series - Fall 2015, November 2015.

REPORT DOCUMENTATION PAGE

Form Approved
OMB No. 0704-0188

1. REPORT DATE *(DD-MM-YYYY)*	2. REPORT TYPE	3. DATES COVERED *(From - To)*
01–02–2018	Technical Memorandum	

4. TITLE AND SUBTITLE

Sandwich Structure Risk Reduction in Support of the Payload Adapter Fitting

5a. CONTRACT NUMBER

5b. GRANT NUMBER

5c. PROGRAM ELEMENT NUMBER

6. AUTHOR(S)

A.T. Nettles, J.R. Jackson, and W.E. Guin

5d. PROJECT NUMBER

5e. TASK NUMBER

5f. WORK UNIT NUMBER

7. PERFORMING ORGANIZATION NAME(S) AND ADDRESS(ES)

George C. Marshall Space Flight Center
Huntsville, AL 35812

8. PERFORMING ORGANIZATION REPORT NUMBER

M–1452

9. SPONSORING/MONITORING AGENCY NAME(S) AND ADDRESS(ES)

National Aeronautics and Space Administration
Washington, DC 20546–0001

10. SPONSORING/MONITOR'S ACRONYM(S)

11. SPONSORING/MONITORING REPORT NUMBER

NASA/TM—2018–219849

12. DISTRIBUTION/AVAILABILITY STATEMENT

Unclassified-Unlimited
Subject Category 24
Availability: NASA STI Information Desk (757–864–9658)

13. SUPPLEMENTARY NOTES

Prepared by the Damage Tolerance Assessment Branch, Engineering Directorate, Marshall Space Flight Center, Huntsville, AL 35812

14. ABSTRACT

Reducing risk for utilizing honeycomb sandwich structure for the Space Launch System payload adapter fitting includes determining what parameters need to be tested for damage tolerance to ensure a safe structure. Specimen size and boundary conditions are the most practical parameters to use in damage tolerance inspection. The effect of impact over core splices and foreign object debris between the facesheet and core is assessed. Effects of enhanced damage tolerance by applying an outer layer of carbon fiber woven cloth is examined. A simple repair technique for barely visible impact damage that restores all compression strength is presented.

15. SUBJECT TERMS

sandwich structure, launch vehicle, scaling, impact damage disbonds, core splices

16. SECURITY CLASSIFICATION OF:			17. LIMITATION OF ABSTRACT	18. NUMBER OF PAGES	19a. NAME OF RESPONSIBLE PERSON
a. REPORT	b. ABSTRACT	c. THIS PAGE			STI Help Desk at email: help@sti.nasa.gov
U	U	U	UU	46	19b. TELEPHONE NUMBER *(Include area code)* STI Help Desk at: 757–864–9658

National Aeronautics and
Space Administration
IS02
George C. Marshall Space Flight Center
Huntsville, Alabama 35812